A Techno-economic Sizing Method for Grid-connected Household Photovoltaic Battery Systems

Yijie Zhang[1], Tao Ma[1]*, Pietro Elia Campana[2], Yohei Yamaguchi[3], Yanjun Dai[1]

[1]*School of Mechanical Engineering, Shanghai Jiao Tong University, Shanghai, China*

[2]*School of Business, Society and Engineering, Malardalen University, Sweden*

[3]*Graduate School of Engineering, Osaka University, Japan*

*Corresponding author: tao.ma@connect.polyu.hk Tel.: +86 21 3420 6056

Abstract: Battery storage provides an effective solution to alleviate the burden of the intermittent photovoltaic production on the grid and increase photovoltaic penetration in residential houses. Despite several existing work dedicated to the evaluation of photovoltaic battery system, the research on system sizing and operation strategy of the household system still has substantial areas to be explored such as techno-economic analysis under different electricity tariffs and comprehensive parametric analyses. In this paper, the mathematical model of a photovoltaic battery system is developed to investigate system performance, based on the various economic and technical indicators. This study demonstrates that the integration of battery energy storage could increase the value of self-consumption and self-sufficiency rates while making payback period longer. Substantial photovoltaic battery systems have been simulated under practical dynamic electricity tariffs in a typical electricity market. Eight cases with different technical performances from the recommended reference combinations are compared and studied in detail. The energy flows among battery bank, grid and household user are discussed, revealing that systems with high self-sufficiency rate lead to more schedulable photovoltaic production, sold electricity and lower battery usage rate than those with high self-consumption rate. Besides, the entire lifecycle economic analysis indicates that a higher self-sufficiency rate refers to higher initial investment but shorter payback period and larger profit. The revenues breakdown of the cases shows that subsidies have a significant impact, especially for cases with high self-sufficiency rate. The levelized cost of electricity of photovoltaic and photovoltaic battery systems ranges from 0.373 to 0.628 CNY/kWh, demonstrating the possibility of partial grid parity under the current situation in Shanghai.

Keywords: Photovoltaic battery system; Self-sufficiency rate; Self-consumption rate; Levelized cost of electricity; Payback period; Distributed energy storage

Nomenclature

C_{annual}	total annual cost of the whole PV battery system (CNY)
C_{bou}	annual bill of electricity bought from the grid (CNY)
$C_{initial}$	initial cost of the construction of PV battery system (CNY)
$C_{O\&M}$	annual operation and maintenance cost of PV battery system (CNY)
$C_{replace}$	annual replacement cost of PV battery system (CNY)
E	electricity (kWh)
E_{usa}	maximum usable electricity of battery discharge or charge for one hour (kWh)
f_{pv}	derating factor of PV production (%/yr)
I	solar radiation (W/m^2)
I_s	solar radiation of the horizontal plane at STC condition, 1000 W/m^2
i	simulation time (hr)
L	whole system lifetime (yr)
m	the minimum year the system starts net benefit (yr)
n	year (yr)
n_{cyc}	battery discharge and charge cycle number
$n_{sto\text{-}life}$	maximum cycle number of battery when selected a typical DOD
P	power (W)
R_b	ratio of direct solar radiation between inclined and horizontal planes
R_{du}	revenue saved by electricity directly supplied by PV production (CNY)
R_{sold}	revenue earned by the electricity sold back to the grid (CNY)
R_{sub}	revenue earned by PV production subsidies (CNY)
T	temperature (K)
t	lifetime (yr)
$t_{battery}$	the lifetime of battery considered both calendar life and cycle life(yr)
$t_{cal\text{-}life}$	calendar life of the battery designed by the manufacturer (yr)
t_{step}	time step of the simulation, assumed as 1 hour
U_L	loss coefficient including all steps of heat transfer loss (W/(m・K))
Y_{pv}	rated installed capacity of PV array (W$_p$)

Greek numbers	
α	absorbance of the PV cell surface
β	inclination angle of PV array (deg), $0 \le \beta \le 90^{\circ}$
γ	discount rate (%)
τ	transmittance of the PV cell surface
ρ	reflectance of the ground
η	efficiency (%)
δ	coefficient for the load profile
Subscripts	
a	ambient
b	diffuse radiation on the horizontal plane
bou	electricity bought from the grid
c	solar cell
ch	electricity used to charge the battery
cyc	battery charge and discharge cycle
d	direct radiation on the horizontal plane
dis	electricity discharged by the battery at AC side
dis,dc	electricity discharged by the battery at DC side
load	household load
loss	electricity loss due to transmission, rectification, and inversion
pv	photovoltaic
sf-dis	self-discharge power of the battery
sold	electricity sold to the grid
T	typical plane with the slope of the system
Tot	total radiation of the horizontal plane
0	total radiation outside the atmosphere
Abbreviations	
DOD	depth of discharge
FIT	feed–in-tariff
IRR	internal rate of return
LCOE	levelized costs of electricity (CNY/ kWh)
MPPT	maximum power point tracking
NOCT	normal operating cell temperature (℃)
NPV	net present value (CNY)

PBP	payback period (yr)
PVB	photovoltaic battery
SCR	self-consumption rate
SOC	state of charge
SSR	self-sufficiency rate
STC	standard test conditions
TOU	time-of-use

1 Introduction

The energy crisis, together with the serious environmental problems, accelerates the deployment of renewable energy sources, especially photovoltaic (PV) with an average increasing installation rate of 57.6% during the last five years [1]. Also the PV global weight-average levelized cost of electricity (LCOE) has reached 0.085 USD/kWh, a 77% reduction from 2010 to 2018 [2]. PV has several advantages including of low cost, eco-friendliness, and relatively high efficiency compared to other renewable energies and can be utilized practically [3], while the intermittency and fluctuation of PV output increase the burden on the electric grid, hence the installation of self-consumed distributed PV systems in residential houses is paid more and more attention in recent years. In China, distributed PV systems, taking up 47.3% of the 2018 PV market [4], were recommended in the 13th five-year PV plan (2016-2020) compared to the centralized PV systems. With the judgment that PV electricity is on the verge of grid parity from user side [5] as well as the threat from the subsidy money shortage and curtailment problem [6], the state subsidy reduced rapidly to 0.180 CNY/kWh for distributed PV systems in 2019 in China [7].

The distributed PV production can alleviate the burden on the grid via reducing the household demand, while the large amount of PV production which fluctuates dramatically may cause problems on transmission and even curtailment. For instance, Xinjiang province registered a curtailment rate of 16% and Gansu province reached 10% in 2018 [8]. Hence, the addition of a flexible energy storage system for self-consumed PV household system is of great importance, which not only buffers the mismatch between load and PV production, but also reduces the interaction between the grid and end-user [9]. The distributed rooftop PV system with utility-scale battery is also emphasized in the major trends that drive the energy transition, according to the report on variable renewable energy from the International Energy Agency (IEA) [10].

Photovoltaic battery (PVB) system has received increasing attention in recent years both in the academic and industrial sectors under the hot topic of the distributed energy system in smart grid. Nevertheless, more possibilities for the reformation of the traditional electricity grid and research on the PVB system are under development.

It is widely acknowledged that the LCOE is a reliable indicator to examine whether the grid parity of grid-connected PV systems could be achieved (from PV side) [11-13] or to calculate the average cost of electricity demand from different sources (from the end-user side) [14]. In Ref. [12], the definitions of LCOE for electrical energy storage (EES) were reviewed, indicating that EES could alleviate the mismatch between the diurnal stochastic PV production and the uncertain load demand. Ref. [11] discussed the assumptions, justifications, and degree of completeness to calculate LCOE. The study conducted by Espinoza et al. [13] demonstrates that the LCOE from PV side is less influenced by external factors, including consumption profiles, level of self-consumption and feed-in tariffs (FIT), than other economic indicators. The LCOE for the end-users was discussed in Ref. [14], in which grid injection fee was considered in the cost and the load demand was taken as the numerator instead of the renewable production. Both two methods for LCOE calculation consider the system lifecycle cost and residual value of the devices. Moreover, the grid parity has become the focus with the reduction of PV installation cost and the ebbing of subsidies.

As the revenue of the system is not considered in LCOE, other indicators should be considered to perform a comprehensive economic analysis. Branker et al. [11] concluded the recognized indicators for economic analysis of PV system, including net present value (NPV), internal rate of return (IRR) and LCOE. Payback period (PBP) represents the first year when the NPV reaches zero

[14]. Based on various economic and technical indicators, substantial research has been conducted on system sizing and energy dispatch strategies of PVB system.

In literature, the combination of economic or technical indicators is usually taken as a separate target when optimizing system sizing. A PV sizing approach based on self-consumption rate (SCR) and self-sufficiency rate (SSR) was proposed by Talavera et al. [15] to maximize the direct self-consumption and reduce the grid injection without consideration of economic factors. The research in Ref. [16] simulated different battery sizes for a PV charging station based on PBP and energy balance equations. The optimization model based on the technical and economic (LCOE) indicators was developed to seek the ideal system combination under different scenarios of grid tariffs [17]. A cost-optimal model was proposed to improve the systematic configuration design of PVB system [18]. The optimal size of battery energy storage system in household PV system was calculated by Olazi et al. [19] via minimizing LCOE under different discharge strategies. The PV size in the residential building facades and rooftops was optimized by Fresitas et al. [20] via maximizing self-sufficiency and minimizing net load variance, while neglecting the economic influences. The study in Ref. [21] discussed the sizing of residential PV system based on cost optimization, whereas the technical indicators were not considered. In Ref. [22], three economic indicators including NPV, IRR, and PBP were considered and the optimal PV and battery size with corresponding economic performance were calculated only under the flat electricity tariff. However, limited attention has been paid to the techno-economic sizing of the PVB system.

Although many efforts have been dedicated to the research on energy dispatch strategies, the improvements are dynamic and specific based on different technical contributions. The study conducted by Hassan et al. [23] utilized the advanced interactive multidimensional modelling system to optimize the energy flow of the PVB system under FIT. Ref. [24] employed the forecasting methods of PV system to compare the performance of different predictive control strategies. The asynchronous advantage actor-critic algorithm was utilized in Ref. [25] to control the energy flow intelligently of multiple sub-grids, for restricting the bi-directional energy with the energy internet and the grid, whereas the economic influence was not considered. In Ref. [26], based on an aging-aware model predictive control approach, the control strategy for PVB system was optimized for minimizing the utility and battery life-cycle costs, however, authors did not consider the scenario of energy sold back to the grid. Despite the various energy dispatch strategies, the strategy that utilizes the load fulfillment priority (PV, battery, grid) and battery charging priority (PV, grid) works as the basic one in literature for comparison with other strategies.

Despite existing work by research activities in systematic design and energy dispatch improvement for household PVB system, this topic still remains in the infant stage. And limited attention has been paid on the techno-economic analysis of grid-connected household PVB system as well as the universal sizing methods, that can be widely applied without considering the weighting factors of different indicators. Besides, few studies took the dynamic electricity tariffs into consideration when sizing the PVB system. In addition, some efforts have also been devoted to the dynamic energy dispatch strategies, whereas a basic strategy is commonly used for comparison.

In this paper, the mathematical model of PVB system is developed to investigate the comprehensive system techno-economic performance, considering the external factors including weather conditions, battery self-discharge and seasonal load variance. Substantial system combinations of PV/ PVB systems have been simulated under the TOU, block and feed-in tariffs practically in a typical area in China, and two common-used reference combination figures of sizing are obtained. Eight cases with typical performance of the technical indicators from the reference combination figures have been studied in detail.

The major novelty and contributions of this paper are summarized as follows:

- The relationship between the combination of PV and battery capacities and the techno-economic performance represented by various technical indicators (SCR and SSR) and economic indicators (LCOE and PBP) are quantitatively evaluated under practical dynamic electricity price system, which combines TOU, block pricing tariffs, FIT as well as the existing subsidies without feed-in limit.

- A simple method is proposed to provide the two reference combination figures for sizing PVB systems based on the techno-economic performance of PVB system. This method is applicable to various application contexts.
- The mechanism that determines the techno-economic performance of PV/PVB system is comprehensively understood in detail, through lifecycle analyses and comparison of case studies which have typical combinations of PV and battery capacities with optimal performance in the technical or economic performance.
- Grid parity based on the current electricity market and policy context of Shanghai has been analyzed with the comparison to the practical tariffs, providing effective suggestions for sizing the distributed PV/ PVB systems of policy-makers in this typical area.

2 System description

In this study, the grid-connected photovoltaic battery (PVB) system contains photovoltaic (PV) modules, energy storage system, converter, load, and power grid, as illustrated in Fig. 1. The PV system injects electricity into the household load, battery system, and the grid through the grid-connected converter which integrates with battery controllers and converter. Besides PV production, the load can also be satisfied by battery discharge and grid electricity injection. The lithium-ion battery bank is selected as the energy storage system in this study. Among various types of battery, although lead-acid battery has the lowest price, its lower energy density and fewer charging/ discharging cycles than lithium-ion battery make the lithium-ion battery a more attractive choice for household users [19]. To obtain a higher roundtrip efficiency, the lithium-ion battery is connected at DC side [27].

When it comes to the grid, the system is simulated based on the hypothesis that there is no electricity transmission limit, eliminating the probability of the curtailment of renewable production acceptance and the failure of power supply.

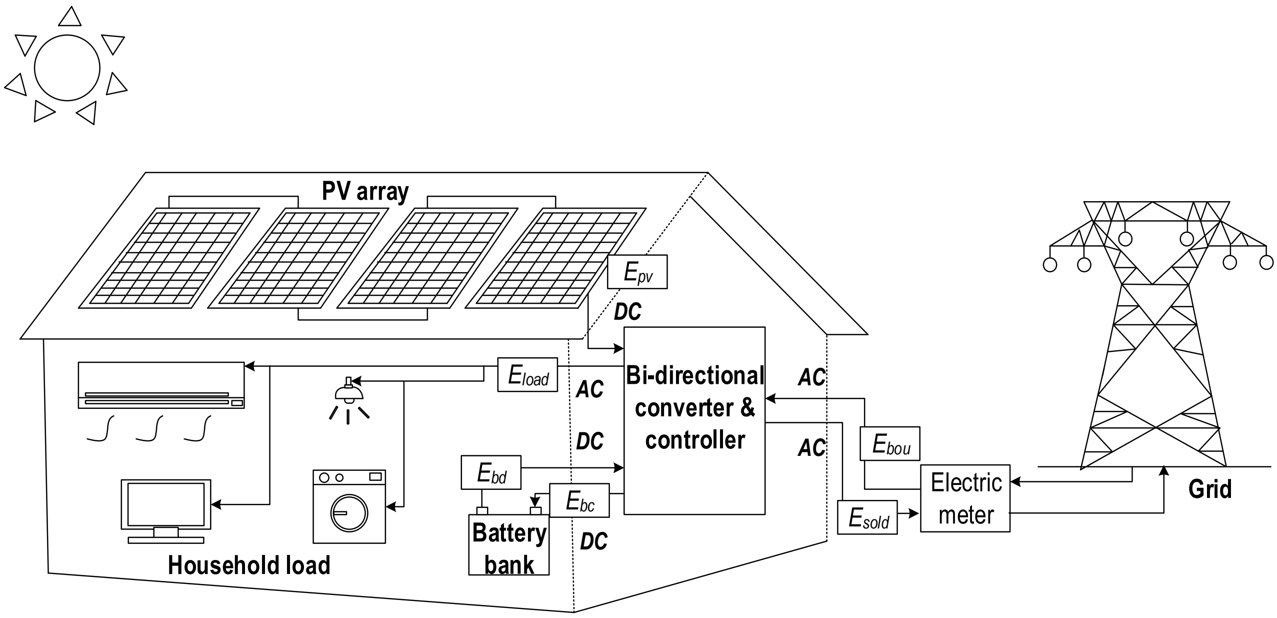

Fig. 1 System configuration of a grid-connected household PVB system

3 Modeling and simulation

3.1 Mathematical Modelling and dynamic electricity market

Energy balance is the core part of any renewable energy based system. As expressed in Eq. (1), the left side of the equation is the electricity conversion, including PV energy E_{pv} (kWh), grid injection E_{bou} (kWh) and battery discharge E_{dis} (kWh), the right side of the equation is the electricity consumption, containing household load demand E_{load} (kWh), battery charge E_{ch} (kWh), electricity sold back to the grid E_{sold} (kWh), and energy loss in different electricity conversion steps E_{loss} (kWh).

$$E_{\mathrm{pv}} + E_{\mathrm{bou}} + E_{\mathrm{dis}} = E_{\mathrm{load}} + E_{\mathrm{ch}} + E_{\mathrm{sold}} + E_{\mathrm{loss}} \tag{1}$$

In this study, the time step of the simulation is one hour due to the time step of the available weather and load data and the relatively long simulation period. The time step of the simulations could be modified according to the various application and different requirements by the decision makers.

3.1.1 PV array

The weather data in Shanghai is provided by SolarGIS [28]. The raw solar radiation data is processed using the radiation conversion model proposed in Ref. [29], which can calculate the solar radiation intensity at an inclined slope based on the global radiation and diffuse radiation of the horizontal plane.

In this study, the PV system is assumed to be installed at 22 °which is considered as the optimal angle for grid-connected PV systems in Shanghai [30]. The total radiation on the inclined PV module can be described as:

$$I_{\mathrm{T}} = I_{\mathrm{b}} R_{\mathrm{b}} + I_{\mathrm{d}} \left(\frac{1+\cos\beta}{2} \right) + I\rho \left(\frac{1-\cos\beta}{2} \right) \quad (2)$$

where I_T is the solar radiation intensity at the inclined slope (W/m^2), I_b is the direct solar radiation intensity at the horizontal plane (W/m^2), R_b is the ratio of direct solar radiation of inclined horizontal planes, I_d is the diffuse solar radiation intensity at the horizontal plane (W/m^2), β is the inclination angle of PV array (deg), $0 \leq \beta \leq 90°$, I is the global solar radiation intensity at the horizontal plane (W/m^2) and ρ is the reflectance of the ground which is assumed as 0.2.

As the weather data only provides the ambient temperature, the temperature of PV module cell T_c (K) is calculated based on the NOCT model [31], as shown below:

$$T_{\mathrm{c}} = T_{\mathrm{a}} + I_{\mathrm{T}} \frac{\tau\alpha}{U_{\mathrm{L}}} \left(1 - \frac{\eta}{\tau\alpha} \right) = T_{\mathrm{a}} + I_{\mathrm{T}} \frac{NOCT - 20}{800} \left(1 - \frac{\eta}{\tau\alpha} \right) \quad (3)$$

where T_a is the ambient temperature (K), τ is the transmittance of the PV cell surface, α is the absorbance of the PV cell surface, U_L is the loss coefficient of heat transfer loss (W/(m K)), η is the efficiency of PV generation (%) and $NOCT$ is the nominal operating cell temperature (℃).

It is assumed that $\frac{\tau\alpha}{U_{\mathrm{L}}}$ is constant and $\tau\alpha$ equals to 0.9 in order to simplify the calculation [32].

After obtaining the solar radiation on the PV module surface, the PV production is simulated using the following equation [33]:

$$P_{\mathrm{pv}} = f_{\mathrm{pv}} Y_{\mathrm{pv}} \frac{I_{\mathrm{T}}}{I_{\mathrm{s}}} \tag{4}$$

where P_{pv} is the PV power (W), f_{pv} is the derating factor (%/yr) including the effects of temperature rise, dust accumulation, wire loss, and PV attenuation, Y_{pv} is the rated installed capacity (W_p), and I_s is the solar radiation of the horizontal plane at standard test condition, set as 1000 W/m^2.

3.1.2 Battery bank

The lithium-ion battery is selected as the energy storage system. The state of charge (SOC) of a battery bank is be described as follows:

$$SOC(i+1) = SOC(i) + P_{\mathrm{ch}}(i) t_{\mathrm{ch}}(i) \eta_{\mathrm{ch}} - \frac{P_{\mathrm{dis}}(i) t_{\mathrm{dis}}(i)}{\eta_{\mathrm{dis}}} - P_{\mathrm{sf\text{-}dis}}(i) \tag{5}$$

where SOC is the state of charge of battery (%), i is the time iteration for almost all of the parameters in the equation (hr), 1≤i≤8760, P_{ch} is the battery charging power (W), t_{ch} is the battery charging duration (hr), assumed as 1 or 0, η_{ch} is the battery charging efficiency (%), P_{dis} is the battery discharging power (W), t_{dis} is the battery discharging duration (hr), assumed as 1 or 0, η_{dis} is the battery discharging efficiency (%), and $P_{sf\text{-}dis}$ is the battery self-discharging power (W).

It is acknowledged that the battery could not be charged and discharged at the same time, the battery charging and discharging duration are limited as follows:

$$\mathrm{t}_{\mathrm{ch}}(i) + t_{\mathrm{dis}}(i) \le t_{\mathrm{step}} \tag{6}$$

where $t_{ch}(i)$ is the battery charging duration (hr), assumed as 1 or 0 in this study, $t_{dis}(i)$ is the battery discharging duration (hr), assumed as 1 or 0 in this study and t_{step} is the time step of the simulation (hr), assumed as 1 in this study.

To prevent the over-charging and over-discharging for a longer lifetime, some constraints are made for the upper and lower limits of SOC [34]:

$$SOC_{\min} \le SOC(i) \le SOC_{\max} \tag{7}$$

where SOC_{min} and SOC_{max} are the lower and upper limits of SOC. It is assumed that SOC_{min} is 0.2 and SOC_{max} is 1.

Battery charging/ discharging power has to be limited as well so as to prevent over-heating [35]. In this study, based on the parameters of the battery provided by the manufacturer [36], the charge and discharge current is assumed to be 25 A. The battery life is not only constrained by the calendar life provided by the manufacturer, but also influenced by the usage condition including cycle number. The cycle number of the battery can be described as follows [18]:

$$n_{\text{cyc}} = \frac{E_{\text{dis,dc}}}{E_{\text{usa}}} \tag{8}$$

where n_{cyc} is the equivalent cycle number for the battery bank, $E_{dis,dc}$ is the battery charging energy on DC side (kWh) and E_{usa} is the maximum battery usable energy during an entire roundtrip (kWh).

Then battery lifetime is the minimum lifetime constrained by calendar life and cycle number [18]:

$$t_{\text{battery}} = \min\left(\frac{n_{\text{sto-life}}}{n_{\text{cyc}}}, t_{\text{cal-life}}\right) \tag{9}$$

where $t_{battery}$ is the minimum lifetime of battery bank (yr), $n_{sto,life}$ is the maximum cycle number of battery bank provided by its manufacturer, $t_{cal\text{-}life}$ is the calendar life of battery bank (yr).

3.1.3 Specification of components

For the convenience of verification of the simulation, the market available products are chosen for the practicability of household users. The typical parameters of components including PV module, inverter, and lithium-ion battery bank are provided in Table 1and Table 2.

Table 1 Parameters for PV and inverter system [37, 38]

PV Array		Grid-connected Inverter	
Parameters	Values	Parameters	Values
Pmax (W_p)	255	Nominal output power at AC side (W_p)	3000
V_{oc} (V)	37.8	Maximum input current of single string (A)	12
I_{sc} (A)	8.95	Voltage range of MPPT (V)	150~550
η (%)	15.67	MPPT efficiency (%)	99.5
K_{pmax} (%/℃)	-0.41	Maximum efficiency (%)	97.5
NOCT (℃)	44	Voltage range of connected battery (V)	42~59
Lifetime (yr)	25	Lifetime of inverter (yr)	10

Table 2 Parameters for battery system [36, 39]

Battery parameters			
Parameters	Values	Parameters	Values
Nominal voltage (V)	48	Calendar Life (yr)	10
Nominal capacity (Ah)	50	Charge voltage range (V)	52.5~54
Discharge voltage range (V)	45~54	Cycle number	>6000 (80% DOD)
Working temperature (℃)	0~50	Battery price ($/kWh)	176

3.1.4 Load profile

The load profile is simulated based on a basic daily load profile with the coefficient considering some daily and monthly randomness. The daily average demand is 11.89 kWh. The coefficient of the load δ_{load} is synthesized based on the following equation [40]:

$$\delta_{load} = 1 + \delta_{day} + \delta_{month} \tag{10}$$

where δ_{day} is the daily randomness and δ_{month} is the monthly randomness of the load profile, assumed as 10% in this study.

The load demand also takes the seasonal variation into consideration on the assumed HVAC load (part of the total load and affects the time people have activity at home) and the load profiles for one typical day and the whole year are displayed in Fig. 2.

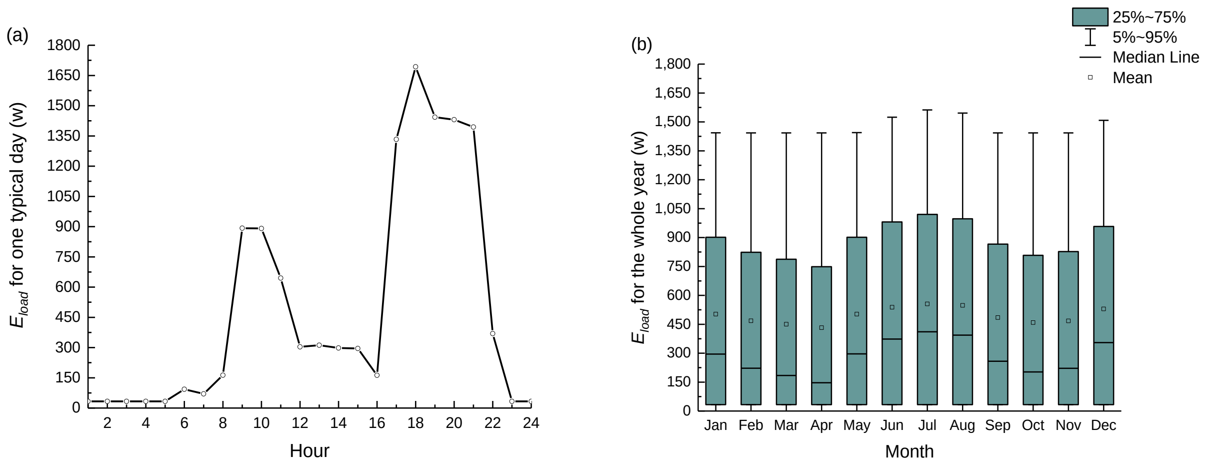

Fig. 2 Load profile: (a) for one typical day; (b) for the whole year.

3.1.5 The electricity market in Shanghai

Due to the local subsidy and dynamic electricity tariffs, Shanghai is considered as a case study in China because its electricity market is representative and relatively developed.

The electricity tariff in Shanghai is dynamic, based on the TOU and block tariffs, as listed in Fig. 3. Usually the consumed electricity during one year in the case study is within the first and second blocks of electricity prices, because less grid electricity is required with the installed PV system.

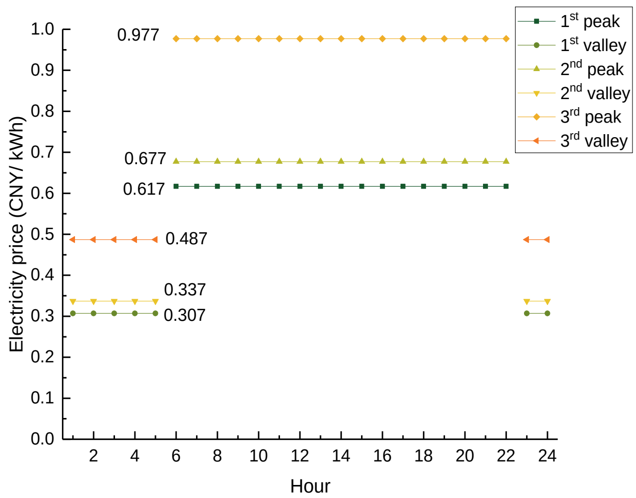

Fig. 3 Electricity purchase prices for residential customers in Shanghai

Besides, for the distributed PV system in Shanghai, the surplus electricity sold to the grid is based on the FIT, and it also receives subsidies from local and central government, as shown in Table 3.

Table 3 State and local subsidies and sell back price for electricity in Shanghai [7, 41]

Electricity price (CNY/ kWh)	Type	Duration
0.180	National whole electricity subsidy price for distributed PV system	2019-2039
0.400	Whole electricity subsidy price for distributed PV system in Shanghai	2019-2022
0.4155	FIT: Electricity sell back price for Shanghai	2017-~

3.2 Indicators for system evaluation

In this study, various technical and economic indicators are utilized to evaluate the performance of the system with different sizes of PV and battery bank. Specifically, technical indicators can describe the system technical performance improvements, such as reliability with the addition of renewable production and energy storage system, while economic indicators focus on the lifetime costs and the revenue of renewable system. Usually these two types of indicators are tradeoff during the decision-making process, hence the paper studies the relationship of the different indicators as well as the impacts on different sizes of PV and battery systems, and summarizes them in a figure as two references for PVB system sizing.

3.2.1 Technical indicators

Self-consumption rate (SCR) and self-sufficiency rate (SSR) are the commonly used technical indicators that demonstrate the time compatibility between renewable production and household usage.

SCR is the ratio of the sum which includes PV production directly used as well as PV production used to charge the battery bank, and total PV generation, focusing on the usage of PV production. SCR can be presented as [42]:

$$SCR = \frac{E_{\mathrm{du}} + E_{\mathrm{ch}}}{E_{\mathrm{pv}}} \tag{11}$$

where E_{du} is the PV direct-used production (kWh), E_{ch} is the PV production injected into the battery bank (kWh) and E_{pv} is the total PV production (kWh).

SSR emphasizes the load demand side, which equals to the proportion of the load demand satisfied by PV power production in total load consumption, as described [43]:

$$SSR = \frac{E_{\mathrm{du}} + E_{\mathrm{dis}}}{E_{\mathrm{load}}} \tag{12}$$

where E_{dis} is the load covered by battery discharge (kWh) and E_{load} is the total load demand (kWh).

3.2.2 Economic indicator

The levelized costs of electricity (LCOE) and payback period (PBP) are two acknowledged and different indicators to evaluate the economic performance of renewable systems.

While the definition of LCOE may vary in different systems and for various purposes [44-46], to discuss the cost of electricity of solar PV and storage system of different sizes, the LCOE for the PV production [12], which includes all parts directly used, sold to grid and stored in battery bank, is selected, instead of the LCOE for end-users [47]. As a result, in this paper the LCOE is the cost of electricity per kWh provided by the PVB system, considering the costs of construction, replacement, operating and maintenance. To calculate it more accurately, the costs of the components are depreciated at the end of the simulation lifetime to prevent overestimation. The LCOE can be calculated through the following equations:

$$C_{\text{annual}}(n) = C_{\text{O\&M}}(n) + C_{\text{replace}}(n) \tag{13}$$

where n is the year number, C_{annual} (n) is the annual cost of the renewable system excluding the grid purchase bill for year n (CNY), $C_{O\&M}$ (n) is the annual operation and maintenance cost of the renewable system for year n (CNY), and $C_{replace}$ (n) is the annual replacement cost of the renewable system for year n (CNY).

$$LCOE = \frac{C_{\text{initial}} + \sum_{n=1}^{L} \frac{C_{\text{annual}}(n)}{(1+\gamma)^n} - C_{\text{sal}}}{\sum_{n=1}^{L} \frac{E_{\text{du,annual}}(n) + E_{\text{sd,annual}}(n)}{(1+\gamma)^n} + \frac{1}{\eta_{\text{ch}}} \sum_{n=1}^{L} \frac{E_{\text{bc,annual}}(n)}{(1+\gamma)^n}} \tag{14}$$

where $C_{initial}$ is the investment of PV and battery systems (CNY), γ is the annual interest rate (%), n is the year number, C_{sal} is the depreciated salvage value of the components (CNY), $E_{du,annual}$ (n), $E_{sd,annual}$ (n), and $E_{bc.annual}$ (n) is the annual energy of direct-used PV production (kWh), sold electricity to the grid (kWh), and battery charge (kWh) for year n with consideration of the degradation of PV generation respectively.

While the LCOE only focuses on the cost of electricity production, another indicator, PBP, that regards both cost and revenue of the whole system, becomes the crucial one to conduct a comprehensive life cycle analysis of the PVB system. The annual revenue equals to the sum of the revenues caused by the saved electricity cost from the direct-use PV electricity, the production subsidies from China and Shanghai, as well as the revenue of electricity sold back to the grid. The *PBP* (yr) can be presented as follow:

$$B_{\text{annual}}(n) = R_{\text{du}}(n) + R_{\text{sold}}(n) + R_{\text{sub}}(n) \tag{15}$$

where B_{annual} (n) is the annual total revenue for PVB system for year n (CNY), R_{du} (n) is the revenue saved by electricity directly supplied by PV production for year n (CNY), R_{sold} (n) is the revenue earned by the electricity sold back to the grid for year n (CNY) and R_{sub} (n) is the revenue earned by PV production subsidies for year n (CNY).

$$PBP = \frac{C_{\text{initial}} + \sum_{n=1}^{m} \frac{C_{\text{annual}}(n)}{(1+\gamma)^n}}{\left\{ \left[\sum_{\text{n}=1}^{m} \frac{B_{\text{annual}}(n)}{(1+\gamma)^n} \right] / m \right\}} \tag{16}$$

where m is the minimum year the total revenue of the system is larger than the total cost (yr).

3.3 Energy dispatch strategy

Energy dispatch is the core part for the energy system with intermittent renewable energy resource and various dispatch components [48, 49]. In this study, a basic energy dispatch strategy is employed and the flow chart of operation principle is depicted in Fig. 4.

When PV generation is higher than the load demand, it will supply the load first, and then the surplus production after meeting the load will charge the battery bank if it is not fully charged. In the end, any further surplus electricity will be sold to the grid based on the FIT policy. When the PV generation cannot meet the load demand, the first priority will be given to the battery discharge if there is available energy, otherwise the household user will purchase electricity from the power grid to cover the net load and maintain the energy balance of the whole system.

It is widely acknowledged that there are other control strategies for the grid connected PVB, such as charging battery using the off-peak grid electricity and optimizing typical indicators from technical, economic and environmental aspects. For better clarity on the various parametric analyses without the impact of different strategies, this study only focuses on this basic strategy (Fig. 4) and more control strategies will be discussed in our future work.

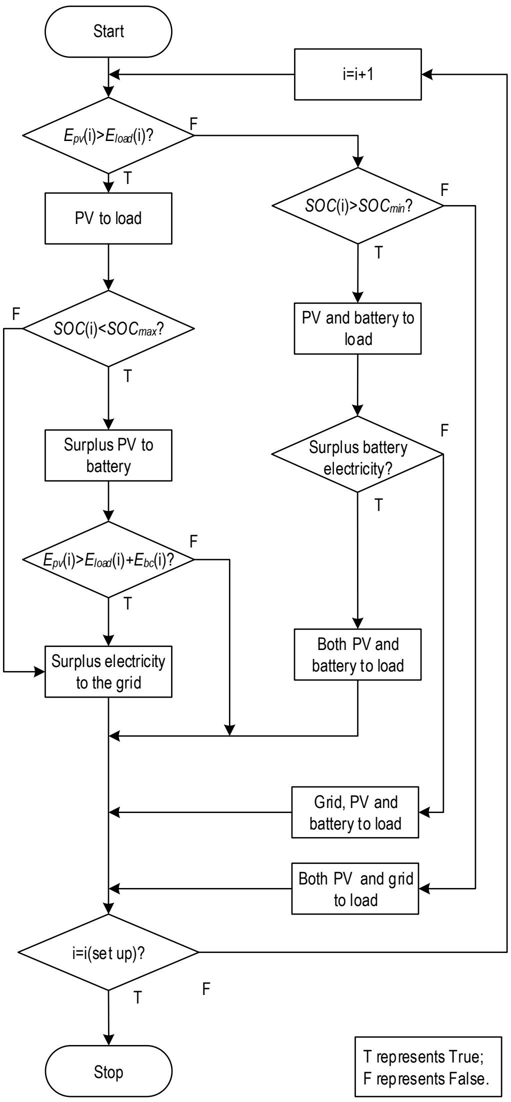

Fig. 4 Flow chart of the energy dispatch strategy in this study

4 Results and discussions

4.1 System simulation and the resultant indicators

Based on the basic energy dispatch strategy depicted in Section 3.3, the yearly simulation and simulation throughout the lifetime of different system combinations of PV and battery bank are conducted, to examine the influence of technical and economic indicators on system sizing. With the consideration of the degradation of PV panels, only the first-year performance of the PV alone or PVB systems is studied in the yearly simulation.

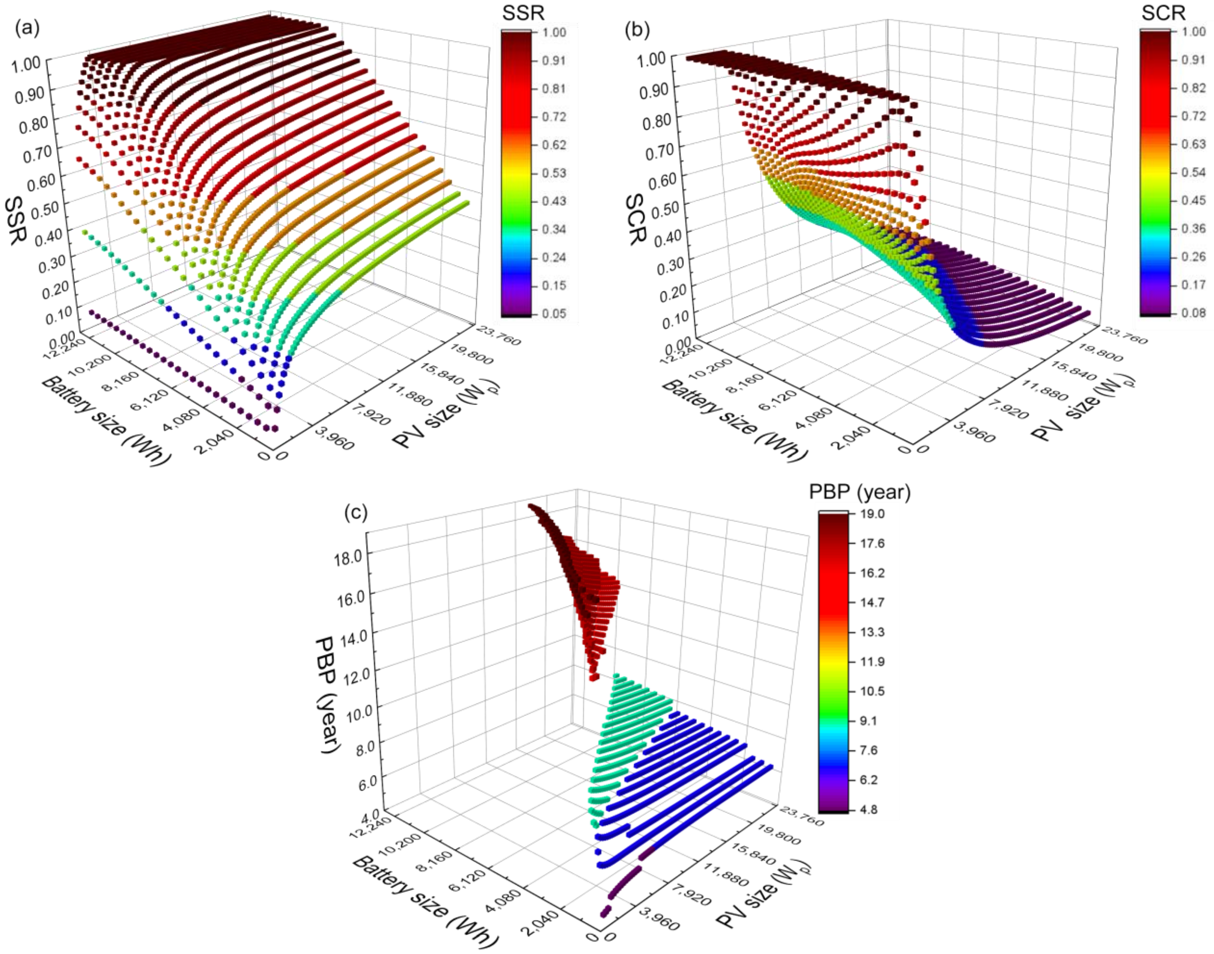

Fig. 5 Performance for different system combinations (rainbow cubes): (a) Self-sufficiency rate performance; (b) Self-consumption rate performance; (c) Payback period performance

Fig. 5 displays the performance matrixes of indicators, SSR, SCR, and PBP, with the variance of PV and battery sizes. SSR and SCR have the same upper limitation, while their trends tend to be different. SSR (Fig. 5 (a)) tends to represent the users' side, which climbs up rapidly with the increase of battery systems under low PV installation, but easily achieves 100% which means the load can be fully covered by PV power output directly or indirectly, when PV and battery systems surpass 2,550 W_p and 8,160 Wh respectively. When it comes to size the system from the user's viewpoint, PV system is recommended to be higher than 2,550 W_p to increase the SSR based on the relatively small increase of PV or battery size, for the insufficient PV production provided by undersized PV system makes the battery bank invaluable and unfavorable with the additional economic consideration.

SCR, as shown in Fig. 5 (b), focuses more on the usage of PV production, which even has the inverse trend with SSR when PV size is too large, meaning the two indicators have their own characteristics from different points of view. By varying the battery size, the relationship between SCR and PV sizes tends to be similar to that of SSR and PV sizes. The upper limitation is reached by the systems with the PV size smaller than 3,825 W_p. The SCR varies more significantly with the PV size increase when battery size is relatively low. From the side of renewable production better usage, the larger battery size is required with the PV size increase to raise the PV production usage, whereas the impact of the battery size increases with the reduction the PV system.

When it comes to the economic indicator, PBP (Fig. 5 (c)), the results can be distributed into two regions, one is from 4.8 years to 9.0 years with intensive system combinations and the other one is from 14.6 years to 19.0 years with decentralized distribution, due to the subsidy change after 15 years. The local subsidy only lasts for 5 years, which is much higher than the subsidy from the central government, and the calendar lifetimes of the battery bank and inverter is 10 years. Thus, if the total cost of the system could not be covered by the total revenue in the first 10 years, the PBP of the system combinations could not be reached within 20 years when the salvage value is not subtracted. The lack for the PBP (rainbow cubes) of some system combinations in Fig. 5(c) represents the scenario that the systems could not earn profit within the assumed lifecycle time, 20 years. The limited increase of revenue caused by increasing battery size could not offset the additional cost of a battery system, as demonstrated by the non-convex lines for each battery size.

System sizing tends to find the systems with best performances both technically or economically, whereas the method based on techno-economic analysis is rarely studied in the previous papers. The common method is to integrate the typical economic and technical indicators with weighting factors, whereas the results of the optimal system sizes vary dynamically and are influenced by the assumed weighting factors to a large extent. Hence, the objective of the system sizing in this paper based on the techno-economic method is to achieve the lowest PBP, based on the targeted SCR or SSR, neglecting the influence of weighting factors.

4.2 System sizing with technical and economic indicators

In this section, the optimal system configurations are discussed, based on the techno-economic evaluation of PBP and SCR/SSR ranging from 0.01 to 1.00 with an interval of 0.01. As shown in Fig. 6 and Fig. 7 respectively, due to the discrete simulation with an interval of the PV and battery systems, some system combinations, which satisfy the typical technical performances, lack the corresponding PBP target, meaning that no payback time is achieved during their life cycle.

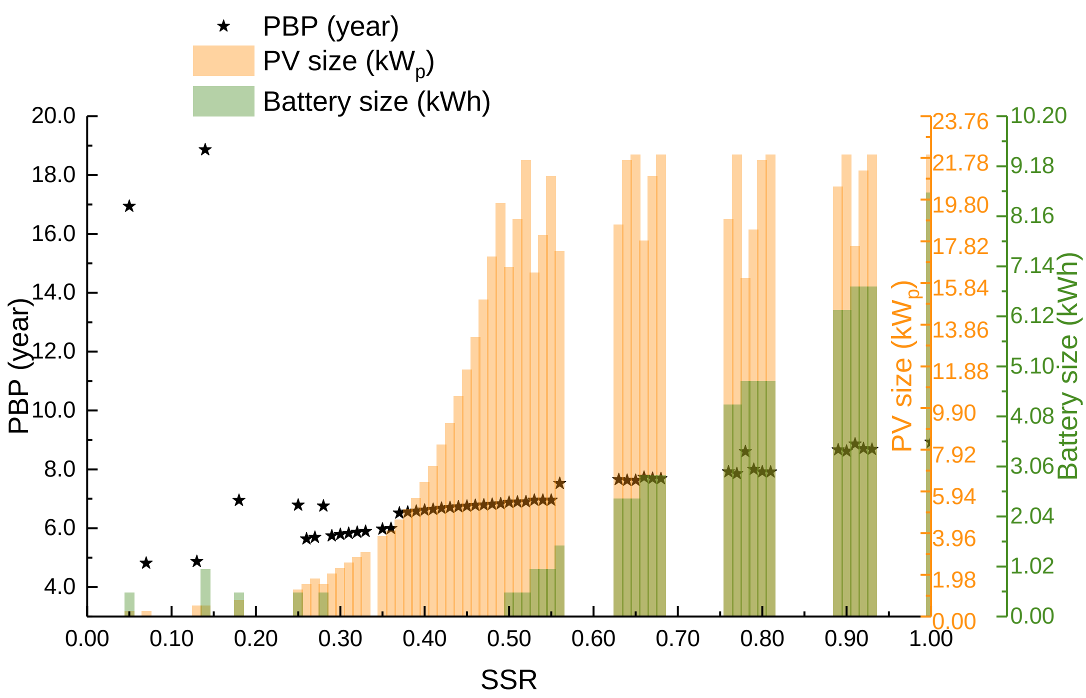

Fig. 6 Optimal sizes under the evaluation of lowest PBP under different targeted SSR

From the household users' point of view, the most cost-efficient system combination in terms of SSR tends to have some patterns, especially when SSR is over 0.28. Based on SSR in Fig. 6, the pattern could be roughly sorted into three regions: chaotic low SSR region (SSR= 0.05-0.28), fast-rising PV region (SSR= 0.29-0.49), and orderly-rising battery region (SSR= 0.50-1.00).

In the first region, low SSRs are hard to find suitable PV and battery sizes because the small PV production fails to make the cost and revenue even, the PV and battery sizes of the system combinations distribute disorderly, and for some SSR values, even no combination of PV and battery bank can be found. Whereas for the second region, SSR climbs quickly with the sharp increase of PV size from 1,530 W_p to 19,635 W_p and the battery size remains 0 for the sake of better economic performance. When SSR should be further increased, the battery bank is added to further raise the proportion of renewable production in the entire household demand in the third region. Battery, though improves the technical performance, the additional cost of step-by-step battery size increase leads to the steadily climbing PBP, in order to match the incremental SSR.

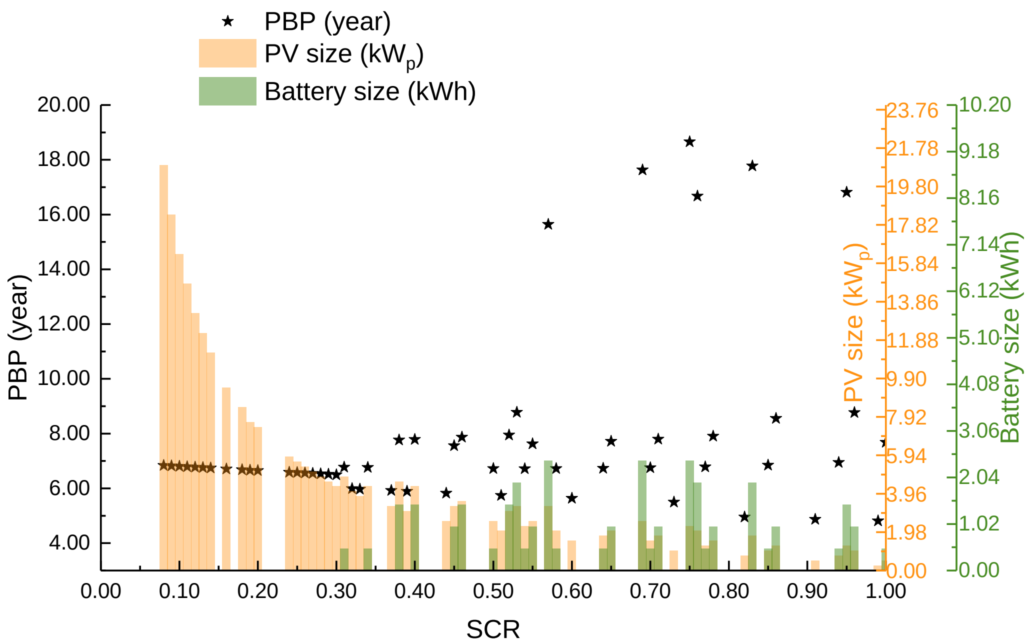

Fig. 7 Optimal sizes under the evaluation of lowest PBP under different targeted SCR

As for the self-consumption of PV production, the technical performance is strongly influenced by the household demand, which is assumed as constant in this study for better comparison. The limited demand constraints the PV size which directly impacts the PV output, the denominator of the SCR. The SCR figure (Fig. 7) could also be separated into two regions: PV rapid decline region (SCR= 0.01-0.30) and disorder PBP region with various battery sizes (SCR= 0.31-1.00).

In the first region, low SCR prefers PV alone system to have better economic performance by increasing the direct-use part of PV production, and the PBPs of the systems fluctuate slightly from 6.50 year to 6.8 year, under the low self-usage demand of PV production. Along with the SCR increase, PV size tends to be reduced to satisfy the higher self-consumption requirement. When it comes to the second region, the improvement of SCR through increasing direct use of PV output might not be so effective; instead, it could be achieved by the addition of a battery storage system, which can offset the time mismatch of load and PV production. However, the addition of battery bank in the system will increase total cost and sacrifice economic performance. In order to fulfill the targeted SCR, battery size increases with almost the same PV size but decreases with the reduction of PV size, which leads to PV and battery size varying, therefore there is great fluctuation in PBP.

In summary, when sizing the PVB system, the optimal PV and battery sizes can be found from Fig. 6 or Fig. 7, based on the users' point of view or better self-consumption of PV production, respectively.

4.3 Case study

To examine the system performance from technical and economic views, eight systems with different SCR/ SSR performances are selected to demonstrate the energy flow and economic results based on the two reference combination figures taken from section 4.2. The eight systems are categorized based on four SSR and SCR values, as displayed in Table 4 and Table 5.

According to Table 4 about the characteristics of the optimal sizes considering SSR and PBP, four typical sizes are selected including one PV alone system and one PV system with the lowest battery size in the second region of Fig. 6, and two PVB systems with moderate battery sizes in the third region of Fig. 6. For a better comparison of two reference combination figures, the sizes of the selected system combinations have similar battery capacities and values of SCR/ SSR.

Table 4 Optimal system combinations based on different SSR and lowest PBP

SSR	PBP (year)	PV size (W_p) /no. of PV modules	Battery bank size (Wh)	LCOE (CNY/kWh)
0.31	5.8	2,550/10	0	0.354
0.50	6.9	16,575/65	480	0.373

0.68	7.7	21,930/86	2,880	0.385
0.92	8.7	21,165/83	6,720	0.407

Table 5 Optimal system combinations based on different SCR and lowest PBP

SCR	PBP (year)	PV size (W_p) /no. of PV modules	Battery bank size (Wh)	LCOE (CNY/kWh)
0.30	6.5	4,335/17	0	0.354
0.50	6.7	2,550/10	480	0.392
0.69	17.6	2,550/10	2,400	0.478
0.95	16.8	1,275/5	1,440	0.500

4.3.1 Technical simulation result for typical sizes of the systems in Shanghai

(a). Technical performance of the selected systems

As for the hourly technical performance of eight cases, the two cases with the highest values of SCR/SSR from the selected cases are studied for further discussion. The hourly energy flow during one year is depicted in Fig. 8 and Fig. 9. The direct-used energy of renewable system for the typical two cases is presented in Fig. 8, demonstrating that PV size is the crucial factor.

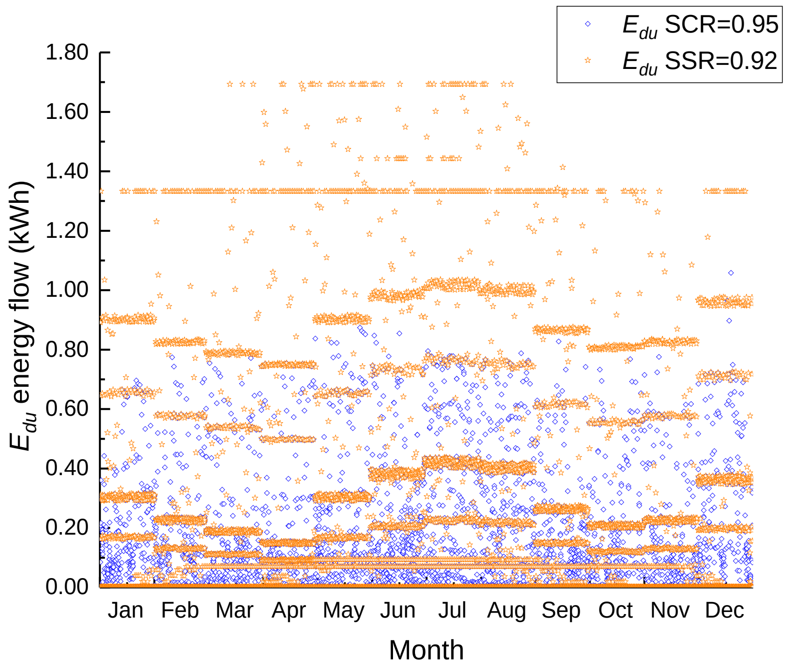

Fig. 8 Direct used energy flow under different SCR and SSR cases

With the extremely high PV production in the high SSR value case (SSR=0.92), the direct-used energy of the case converges typical platforms (the line segments that orange points constitute) for each month, which are almost the same as the load demand in the daytime. Several energy flows of the case (SSR=0.92) scatter below the orange line segments set by the load demand, due to the insufficient solar radiation at night or typical hours in daytime. The higher direct-used energy flows are usually provided by larger PV capacities leading to higher SSR value, while higher SCR value, which emphasizes the higher consumption rate of PV production, may not lead to the increase of direct-used energy. Hence, the direct-used energy of the other case (SCR=0.95) assemble mostly under 0.20 kWh and spread between 0.20 and 1.00 kWh.

Although it is acknowledged that PV production has a definite relationship with solar radiation, the converging platforms for each month in Fig. 8 are mainly due to the assumed load demand for PV production of case SCR=0.95 is far more than the total load.

The mutual energy flows between the prosumer and the grid of the two cases in the first year without the consideration of degradation are depicted in Fig. 9.

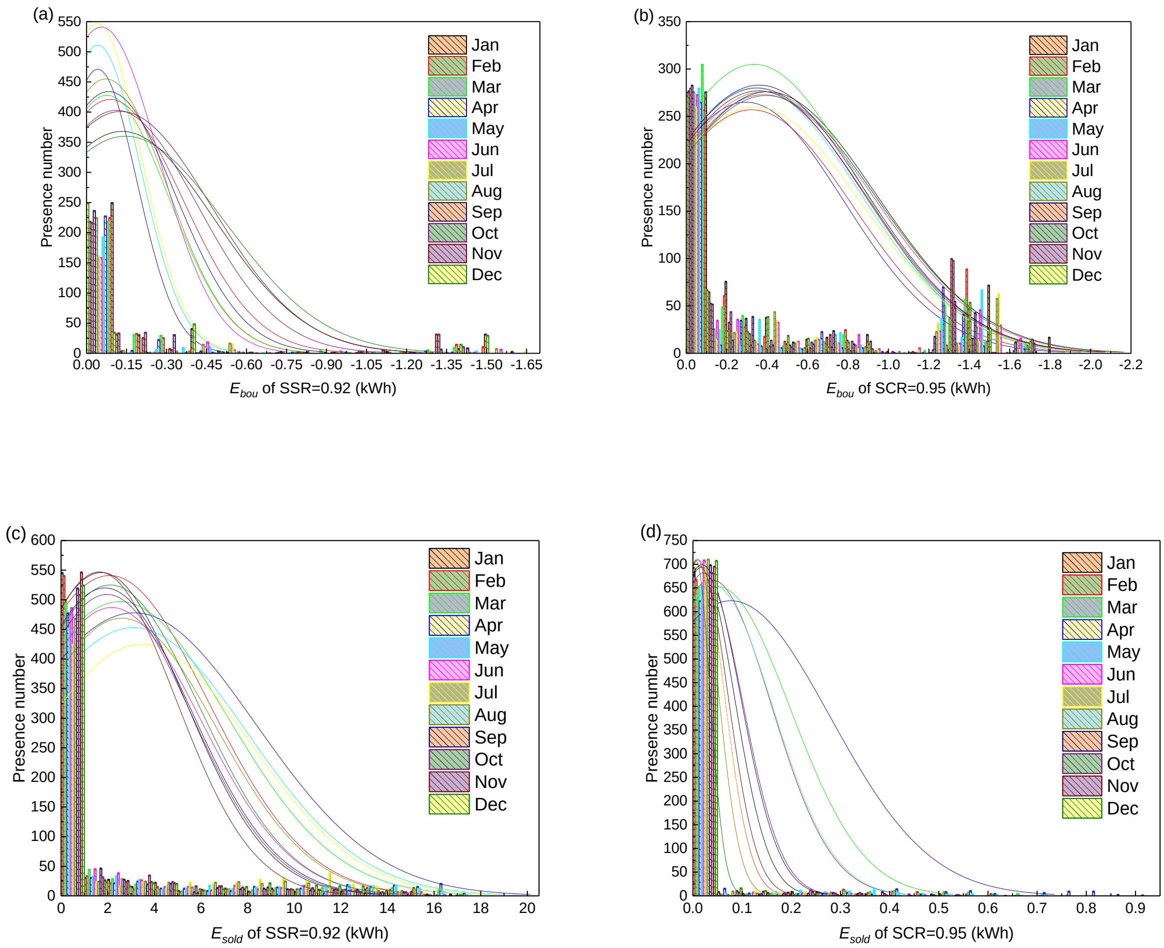

Fig. 9 Technical performance of SCR and SSR cases of energy flow with the grid: (a) E_{bou} of case SSR=0.92; (b) E_{bou} of case SCR=0.95;(c) E_{sold} of case SSR=0.92; (d) E_{sold} of case SCR=0.95.

With the sufficient PV production and relatively large battery storage, the grid injection of case (SSR=0.92) has been cut down sharply and the distribution lines of each month reach the summit before 0.20 kWh, while the distribution lines of the other case (SCR=0.95), with less PV and battery capacity, reach the summit at around 0.40 kWh with the consideration of monthly load demand and PV production variation. The hourly purchased electricity of the case with SCR value of 0.95 distributes more evenly and in a larger region than that of the other case (SSR=0.92).

Moreover, the sold electricity to the grid of the case (SSR=0.92) displays the monthly variance of the surplus renewable production after load satisfaction and battery charge. While the insufficient solar radiation in June prevents it from more sold electricity to the grid, the months in spring and summer with better radiation conditions are prone to sell more energy to the grid, thus gaining higher revenues. Due to the low PV production as compared to the consumption, the other case (SCR=0.95) does not present the energy flow sold back to the grid obviously and the distribution lines reach the summit before 0.10 kWh in autumn and winter months.

The hourly energy flows in two typical days (sunny and cloudy) of the case with 0.92 SSR value are presented in Fig. 10.

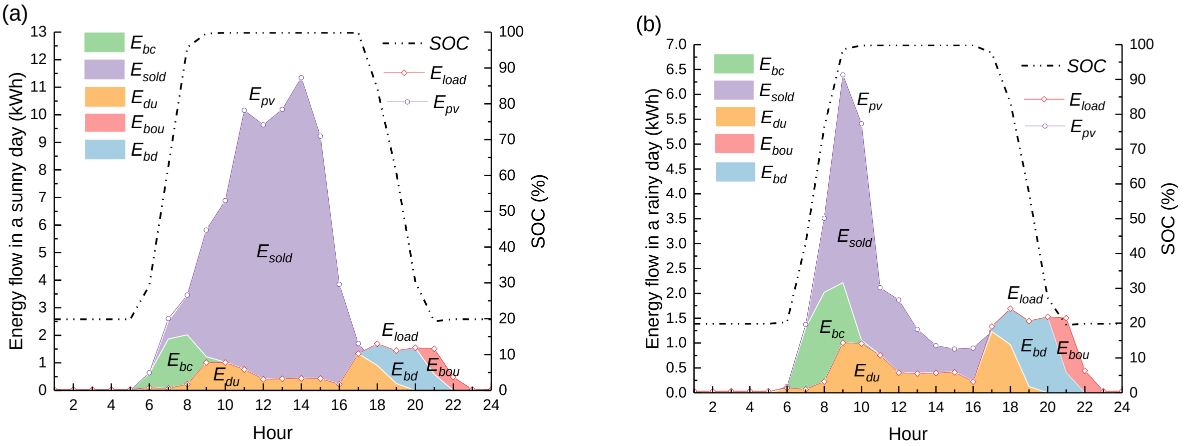

Fig. 10 Hourly energy flows for two typical summer days of case SSR=0.92: (a) sunny day; (b) cloudy day.

It can be seen that the hourly energy flows including PV production (E_{pv}), direct-used PV production (E_{du}) and energy sold to the grid (E_{sold}) of the two days are obviously different, especially after 10 am. However, the daily PV production of the cloudy day is still plentiful, for the two selected days both have adequate solar radiation and the PV size (21,165 W_p) of the case SSR=0.92 is extremely large. As the total PV production is plentiful, the curves of the two battery SOC are similar and the difference of the two energy flows bought from the grid (E_{bou}) is not significant.

To further analyze the technical performance of the two typical systems, the average daily energy flows have been plotted in Fig. 11. With higher PV installation, the average daily PV production of the case with high SSR is much larger than that of the other case (SCR=0.95), providing more schedulable surplus electricity after satisfying the load. However, due to the smaller PV size of the case with high SCR, the battery charge and discharge flows are sharply reduced compared to that of the other case (SSR=0.92). Meanwhile, the sold electricity of the case with 0.92 SSR value is much higher than the other one (SCR = 0.95), which may unfortunately increase the burden on transmission with the grid.

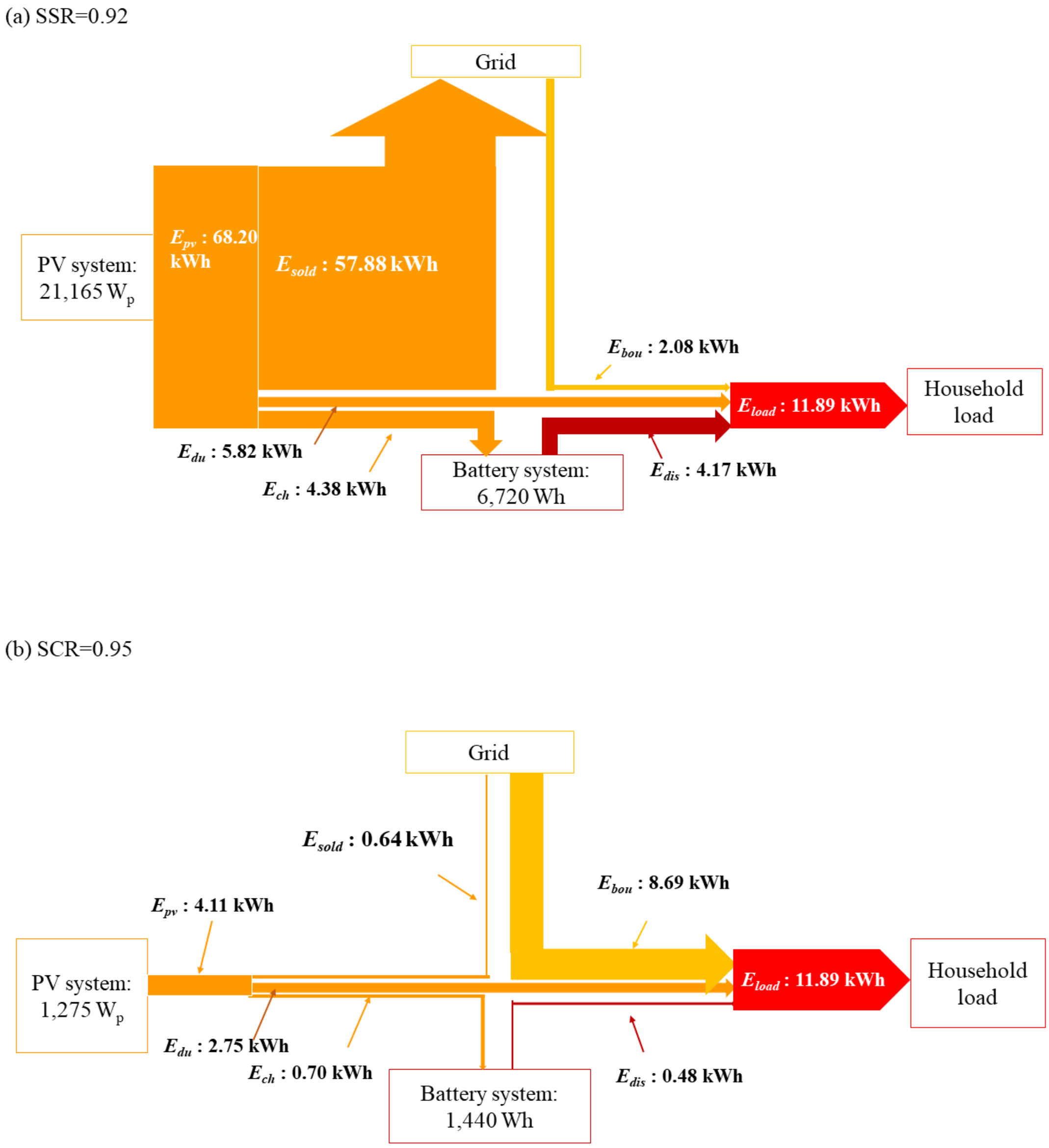

Fig. 11 Average daily energy flow of the representative cases: (a) SSR = 0.92; (b) SCR = 0.95.

(b). Battery bank SOC

The SOC performance of the six PVB systems is compared in Fig. 12. For SSR focuses on the satisfaction of load demand, the battery size tends to decrease and thus the usage frequency of the battery prone to increase compared with the systems with different SCRs. If the system is designed from the viewpoint of renewable production usage (higher SCR value), the over-sized battery size will be recommenced, therefore the battery bank will have a lower depth of charging/discharging under the assumed constant household demand. With the increase of SCR, the battery bank SOC grows lower which is more easily to be influenced by the lack of solar radiation and the battery usage rate tends to drop.

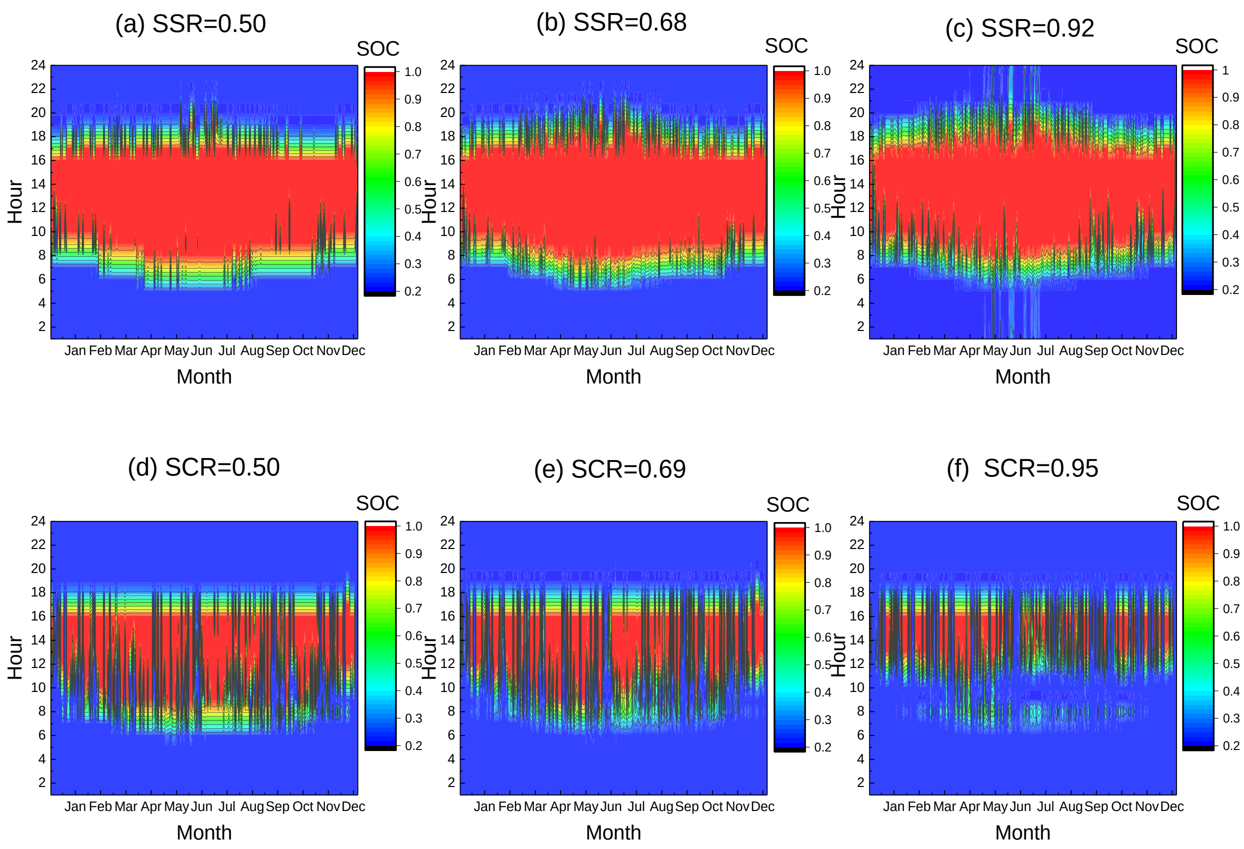

Fig. 12 SOC rainbow of the typical systems

(c). Energy balance analysis

The yearly energy flows of the eight cases including E_{pv}, E_{du}, E_{bc}, E_{bd}, E_{load}, E_{bou}, and E_{sold} is depicted in Fig. 13, especially presenting the comparison of E_{pv} and E_{load}.

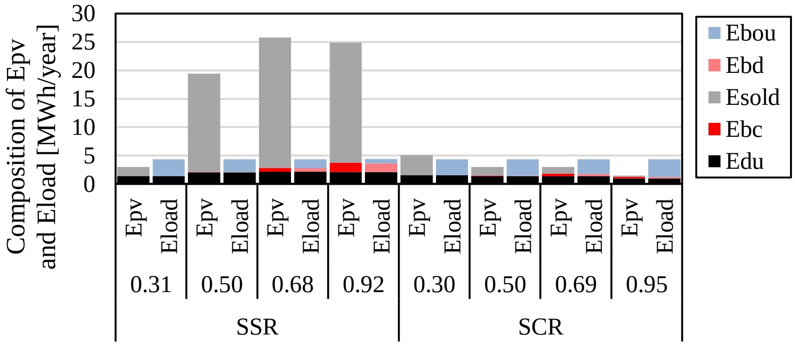

Fig. 13 Yearly energy flow for the selected systems

It can be seen that with the increase of PV capacity, the sold electricity (grey part) increases dramatically and the purchased electricity (blue part) decreases sharply, while the direct-used energy increases until the value meets load demand together with the selected battery storage. When it comes to the performance of battery system, the system emphasizes the renewable energy usage (SSR over 0.31) tends to have larger battery storage flows (red and pink parts) to fulfill the electricity need that does not match the PV profile. On the other hand, the SCR of systems recommended for the satisfying self-consumption (SCR over 0.30) can be even raised both through increasing the battery size and decreasing PV production.

4.3.2 *Economic analysis*

4.3.2.1 Cash flows for typical PV alone and PVB systems

To illustrate the economic performance of PV alone and PVB systems, the net present value (NPV) and the discounted cash flows, are commonly utilized. The larger value of NPV represents larger economic profits [50]. The discounted cash flows and NPV for the selected systems throughout the system lifetime are presented in Fig. 14. The first cross point of the discounted cash flow curve with the zero line demonstrates when the total cost could be completely covered by the total revenue at the first time, namely PBP. The cash flows not only take the initial cost and the costs of operation, maintenance as well as replacement into consideration, but also consider the revenues from subsidies, reduction of electricity bill and sold electricity. Therefore, the sizes of PV and battery systems, which influence the lifecycle costs and various revenues largely, become the dominant factors under the typical practical electricity market.

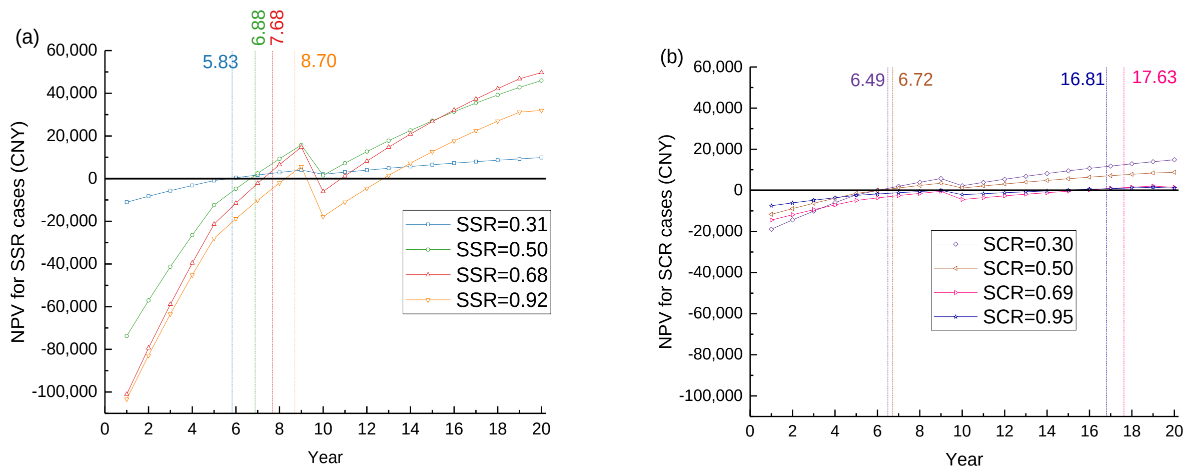

Fig. 14 Cash flow for selected PV alone and PVB systems: (a) four SSR cases; (b) four SCR cases.

As for the different cases selected based on the indicator of SCR or SSR with the lowest PBP, the cash flows of the cases vary dramatically. Moreover, the eight cases can approximately be divided into two groups according to the curves of discounted cash flow. The first group includes the systems with large PV size and relatively large battery storage (SSR=0.50, SSR=0.68, SSR=0.92) and the other one contains small PV size and small or none battery addition (SSR=0.31, SCR=0.30, SCR=0.50, SCR=0.69, SCR=0.95).

The first group invests higher initial capital to purchase a larger PV system as well as the matched battery bank, at the same time they can receive higher revenues, therefore achieving lower PBP and more competitive NPV. In contrast, although the later one invests much lower initially, the lower PV size and battery capacity of the second group make the discounted cash flows within the lifetime much lower and PBP differs depending on the matching rate of battery and PV sizes.

With the consideration of the local subsidy in Shanghai in the first five years, the curves of NPV climbs quite quickly in this duration, narrowing the values of PBPs (the cross points with zero line) of PVB systems with small battery bank.

4.3.2.2 Revenues breakdown of representative PV alone and PVB systems

A detail breakdown of the revenues from various sources, including those from the saved electricity bill (R_{saved}), the sold electricity (R_{sold}), and the subsidy from local (first 5 years) and central (20 years) governments which contains the subsidy earnings in the first 5 years ($R_{sub5yrs}$) and the latter 15 years ($R_{sub15yrs}$) is given in Fig. 15. The size of the pies reflects the total amount of revenues.

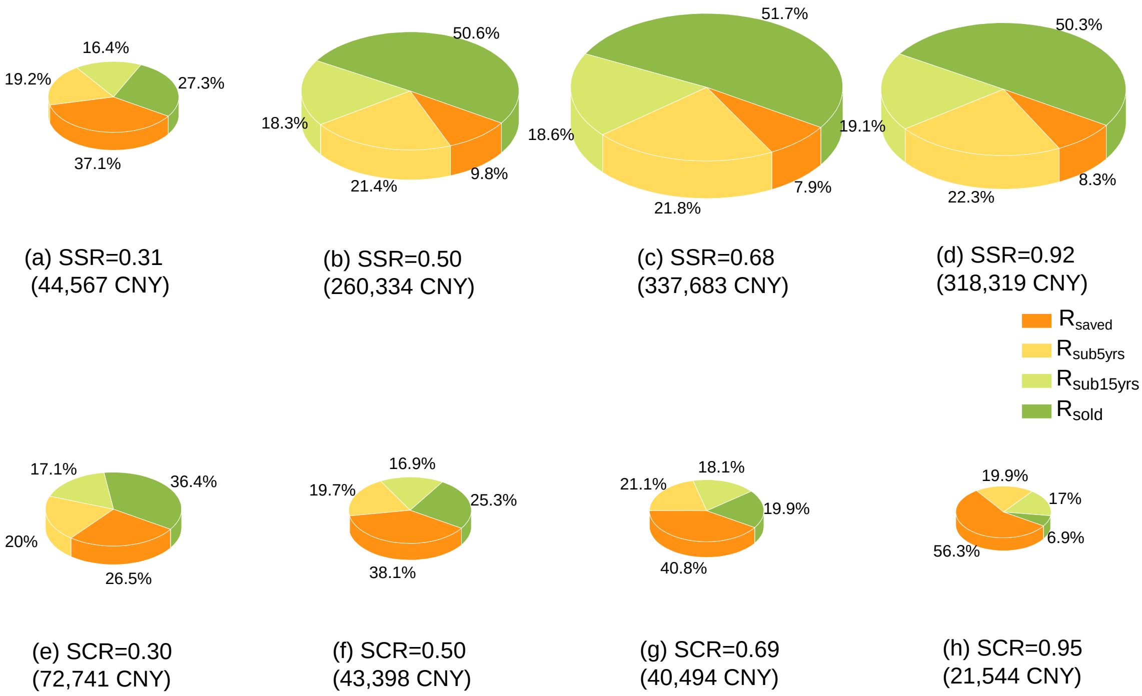

Fig. 15 Revenues breakdown for selected PV and PVB systems

The revenue earned by selling electricity to the grid is largely impacted by the PV size, and its share varies from 6.9% to 51.7% with different SCR and SSR. Generally, larger share of this part leads to higher SSR or lower SCR.

As for the revenue by saving electricity bill via PV directly consumption, the PV size also influences the share largely while the household load limits the bill within 26,629 CNY despite the further increase of PV size. The share of this part decreases with the increase of SSR (usually PV size also climbs up), whereas this share increases when SCR rises as PV size decreases and battery size increases, leading to the further fulfillment of load demand that cannot be covered by direct PV production.

When it comes to the remaining shares of the revenue, the subsidy has a direct positive relationship with the PV installation. The subsidy for the first five years, which is mainly contributed by the local subsidy in Shanghai, takes larger share than that of the rest fifteen years contributed rarely by the lower state subsidy, demonstrating the obvious influence of the subsidy change in the current situation. For PV size has a larger impact on SSR value than SCR value, the subsidy change acts as a more dominant factor of SSR.

4.4 Grid parity of PV generation for different sizes of systems

To describe the grid parity in the current market situation of Shanghai, the LCOEs for different system combinations are displayed in Fig. 16. The LCOE in this paper focuses on the cost of renewable conversion, which contains the lifecycle cost and renewable production for PV and battery systems.

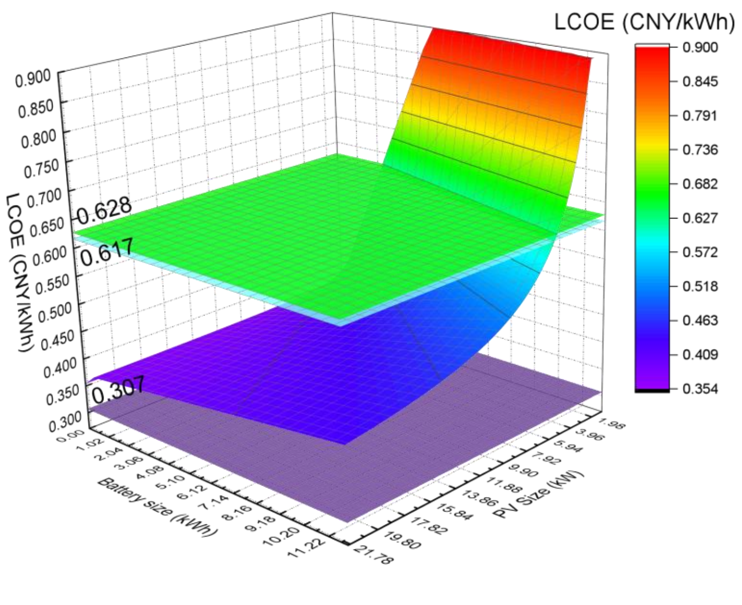

Fig. 16 LCOE for different sizes of PV alone and PVB systems

Taking the lowest block tariff of grid electricity price system as the boundary, that is 0.617 CNY/kWh (middle blue plane) and 0.307 CNY/kWh (lower purple plane) in the practical TOU tariff, the results of the LCOE for different PV and PVB systems are compared with the boundaries vividly. In addition, the average electricity price for the assumed load demand, which is 0.628 CNY/kWh, is presented as the upper green plane in Fig. 16. The minimum LCOE for the all system combinations is 0.354 CNY/kWh for the PV alone system, meaning that the production cost of PV output is still less economical compared with the lowest valley grid electricity price. Most of the LCOEs range from 0.373 to 0.628 CNY/kWh and vary stepwise with the growth of PV installation and battery addition, except for the LCOEs that are over the blue plane (0.617 CNY/kWh) with relatively high battery size (larger than 480 Wh) and low PV size (smaller than 5,610 W_p). The LCOEs of the selected systems are displayed in Table 4 and Table 5.

Under the current situation of the electricity market in Shanghai, the LCOEs for PV and PVB systems tend to be competitive with the peak electricity price but not so profitable compared to the valley electricity price. This means that the grid parity could be partly achieved and the PV production could be more attractive with the gradual increase in grid electricity price and decrease of the system costs in the near future.

5 Conclusions

In this paper, the grid-connected photovoltaic battery (PVB) system is simulated under the dynamic practical electricity tariffs to analyze the performance of different system combinations on various technical and economic indicators, which could be a comprehensive reference of sizing optimization based on the various parameters.

Two applicable reference combination figures of sizing, obtained from the viewpoints of energy sufficiency (self-sufficiency rate (SSR)) and renewable energy usage (self-consumption rate (SCR)), considering the lifecycle economic profit, have been discussed. As for the decision makers, PVB system could be obviously more favorable in terms of the technical performance than photovoltaic (PV) alone system whereas less profitable especially with small PV installation. The influence of the battery bank on the SSR/SCR is largely related to the PV size.

Eight detailed cases with different technical performances have been studied to analyze the energy flows and cash flows throughout the system lifecycle. The results demonstrate that high SSR seekers tend to have the opportunity to schedule more renewable production, more battery storage electricity, sell more electricity and obtain higher lifecycle profits, whereas leading to higher transmission burden on the power grid and higher initial investment than high SCR seekers. The analyses also indicate that decision makers focus on the renewable energy consumption prone to have relatively high battery usage rate and long payback period.

When it comes to the subsidy impact, the decision makers emphasize the sufficiency of the load demand will be more influenced compared with those focus on better renewable energy usage. Besides, the local subsidy in the short period of the typical area affects the profits to a large extent.

The battery bank increases the levelized cost of electricity (LCOE) of the PV system continuously with the increase of the battery size, whereas the increasing rate is lowered by the increased PV size. The grid parity for the residential sector has been partially achieved with the LCOEs ranging mostly from 0.373 to 0.628 CNY/kWh in the current electricity market of Shanghai. Systems with a relatively small battery size (smaller than 480 Wh) and high PV size (larger than 5,610 W_p) can compete with the peak electricity price of the first grade easily, while the valley electricity price of the first grade remains a challenge.

The improvement of energy dispatch strategies, such as strategies under optimization routine and taking predictive data into consideration, as well as the sizing optimization based on smart algorithms such as genetic algorithm will be studied in future work.

Acknowledgements

The authors would appreciate the financial supports provided by National Natural Science Foundation of China (NSFC) through the Grant 51976124, and the Strategic Partnership Fund between Shanghai Jiao Tong University and Osaka University (2019-2021 SJTU-OU). The authors would also like to acknowledge SolarGIS for providing weather data in Shanghai.

References

[1] Renewable Energy Statistics 2019. Abu Dhabi: International Energy Agency; 2019. p. 49.

[2] Renewable Power Generation Costs in 2018. Abu Dhabi: International Energy Agency; 2019. p. 47.

[3] Hosseini-Fashami F, Motevali, A., Nabavi-Pelesaraei, A., Hashemi, S.J., Chau, K.W. Energy-Life cycle assessment on applying solar technologies for greenhouse strawberry production. Renewable and Sustainable Energy Reviews. 2019;116:109411.

[4] Photovoltaic Industry Development Roadmap of China 2018. China Photovoltaic Industry Association; 2019. p. 45.

[5] Jinyue Yan YY, Pietro Elia Campana and Jijiang He. City-level analysisof subsidy-free solar photovoltaic electricity price, profits and grid parity in China. Nature energy. 2019;4:709-17.

[6] IEA-PVPS annual report 2017. International Energy Agency; 2018. p. 57-9.

[7] Commission NDaR. Notice of the National Development and Reform Commission on improving the feed-in tariff mechanism for photovoltaic power generation. http://www.ndrc.gov.cn/zwfwzx/zfdj/jggg/201904/t20190430_935312.html2019.

[8] Operation presentation of grid-connected renewable energies in 2018. National Energy Administration; 2019.

[9] Mansour Alramlawi AG, Erfan Mohagheghi, Pu Li. Optimal operation of hybrid PV-battery system considering grid scheduled blackouts and battery lifetime. Solar Energy. 2018;161:125-37.

[10] Solutions to integrate high shares of variable renewable energy (Report to the G 20 Energy Transitions Working Group (ETWG)). Abu Dhabi: International Energy Agency; 2019.

[11] K. Branker MJMP, J.M. Pearce. A review of solar photovoltaic levelized cost of electricity. Renewable & Sustainable Energy Reviews. 2011;15:4470-82.

[12] Chun Sing Lai MDM. Levelized cost of electricity for solar photovoltaic and electrical energy storage. Applied Energy. 2017;190:191-203.

[13] R. Espinoza a, E.Mu~noz-Ceron b, *, J. Aguilera c, J. de la Casa c. Feasibility evaluation of residential photovoltaic self-consumption projects in Peru. Renewable Energy. 2019;136:414-27.

[14] Tom Terlouw TA, Christian Bauer, Wilfried van Sark. Multi-objective optimization of energy arbitrage in community energy storage systems using different battery technologies. Applied Energy. 2019;239:356-72.

[15] Talavera DL, F.J. Mo-R, G. J-C, C. R-C. A new approach to sizing the photovoltaic generator in self-consumption systems based on cost–competitiveness, maximizing direct self-consumption. Renewable Energy. 2019;130:1021-35.

[16] Ms AE, Norton B, Conlon M. Modelling and Energy Management Optimisation of Battery Energy Storage System Based Photovoltaic Charging Station (PV-CS) for University Campus. 2016.

[17] Marco Bortolini MG, Alessandro Graziani Technical and economic design of photovoltaic and battery energy storage system. Energy Comversion and Management. 2014;86:81-92.

[18] Weniger J, Tjaden T, Quaschning V. Sizing of Residential PV Battery Systems. Energy Procedia. 2014;46:78-87.

[19] Balint D. Olaszi JL. Comparison of different discharge strategies of grid-connected residential PV systems with energy storage in perspective of optimal battery energy storage system sizing. Renewable & Sustainable Energy Reviews. 2017;75:710-8.

[20] S. Fresitas CR, M.C. Brito. Minimizing storage needs for large scale photovoltaics in the urban environment. Solar Energy. 2018;159:375-89.

[21] Juha Koskela AR, Pertti Järventausta. Using electrical energy storage in residential buildings – Sizing of battery and photovoltaic panels based on electricity cost optimization. Applied Energy. 2019;239:1175-89.

[22] Mulder G, Six D, Claessens B, Broes T, Omar N, Mierlo JV. The dimensioning of PV-battery systems depending on the incentive and selling price conditions. Applied Energy. 2013;111:1126-35.

[23] Sani Hassan A, Cipcigan L, Jenkins N. Optimal battery storage operation for PV systems with tariff incentives. Applied Energy. 2017;203:422-41.

[24] Litjens GBMA, Worrell E, Sark WGJHMv. Assessment of forecasting methods on performance of photovoltaic-battery systems. Applied Energy. 2018;221:358-73.

[25] Haochen Hua YQ, Chuantong Hao, Junwei Cao. Optimal energy management strategies for energy Internet via deep reinforcement learning approach. Applied Energy. 2019;239:598-609.

[26] Jie Cai HZ, Xing Jin. Aging-aware predictive control of PV-battery assets in buildings. Applied Energy. 2019;236:478-88.

[27] Klauw TVD, Hoogsteen G, Gerards MET, Hurink JL, Hebner RE. Assessing the potential of residential HVAC systems for demand-side management. 2016 IEEE Power & Energy Society Innovative Smart Grid Technologies Conference (ISGT)2016.

[28] SOLARGIS. Solargis solar radiation data. https://solargis.com/products/evaluate/useful-resources.

[29] Liu BYH. The Interrelationship and Characteristic Distribution of Direct, Diffuse and Total Solar Radiation. Solar Energy. 1960;4:1-19.

[30] Association CPI. Residential grid-connected photovoltaic (PV) system standard series Part 2-2: Design spefications- PV array2019.

[31] Townsend TU. A Method for Estimating the Long-Term Performance of Direct-Coupled Photovoltaic Systems. 1989.

[32] John A. Duffie WAB. Solar Engineering of Thermal Processes. Fourth ed: John Wiley & Sons, Inc.; 2013.

[33] Tao Ma MSJ. Integrated sizing of hybrid PV-wind-battery system for remote island considering the saturation of each renewable energy resource. Energy Comversion and Management. 2019;182:178-90.

[34] Gabash A, Li P. Active-Reactive Optimal Power Flow in Distribution Networks With Embedded Generation and Battery Storage. IEEE Transactions on Power Systems.27:2026-35.

[35] Kalaitzakis EKaK. Novel battery charging regulation system for photovoltaic applications. IEE Proceedings 2004;151:191-7.

[36] PYLONTECH. Product specification of lithium-ion battery storage system for household PV system (US 2000). http://www.pylontech.com.cn/cn/pro_detail.aspx?id=114&cid=23.

[37] Shanghai GGSOLAR Technology Co. L. Product specification and prices for FillmaxGG610P polysilicon PV panel from GGSOLAR http://www.china-nengyuan.com/product/100156.html.

[38] Growatt. Product center for grid-connected inverter of Growatt (SPH series). http://www.growatt.com/show-22-592.html.

[39] BloombergNEF. A Behind the Scenes Take on Lithium-ion Battery Price. https://about.bnef.com/blog/behind-scenes-take-lithium-ion-battery-prices/2019.

[40] Muhammad Shahzad Javed DZ, Tao Ma, Aotian Song, Salman Ahmed. Hybrid pumped hydro and battery storage for renewable energy based power supply system. Applied Energy. 2020;257:114026.

[41] Measures of Shanghai municipality on special fund support for the development of renewable energy In: commission Sdar, editor.2019.

[42] Alejandro Pena-Bello MB, Martin K. Patel, David Parra. Optimizing PV and grid charging in combined applications to improve the profitability of residental batteries. Journal of Energy Storage. 2017;13:58-72.

[43] Nuria Mart ń-Chivelet DM-G. Optimizing photovoltaic self-consumption in office buildings. Energy & Buildings. 2017;150:71-80.

[44] Branker K, Pathak M, Pearce JM. A Review of Solar Photovoltaic Levelized Cost of Electricity. Social Science Electronic Publishing. 2011;15:4470-82.

[45] Pawel, Ilja. The Cost of Storage – How to Calculate the Levelized Cost of Stored Energy (LCOE) and Applications to Renewable Energy Generation. Energy Procedia.46:68-77.

[46] Lai CS, Jia Y, Xu Z, Lai LL, Li X, Cao J, et al. Levelized cost of electricity for photovoltaic/biogas power plant hybrid system with electrical energy storage degradation costs. Energy Conversion & Management. 2017;153:34-47.

[47] Tom Terlouw TA, Christaun Bauer, Wilfries van Sark. Multi-obkactive optimization of energy arbitrage in community energy storage systems using different battery technologies. Applied Energy. 2019;239:356-72.
[48] Ma T, Yang H, Lu L. A feasibility study of a stand-alone hybrid solar–wind–battery system for a remote island. Applied Energy. 2014;121:149-58.
[49] Ma T, Yang H, Lu L, Peng J. Technical feasibility study on a standalone hybrid solar-wind system with pumped hydro storage for a remote island in Hong Kong. Renewable Energy. 2014;69:7-15.
[50] S. Schopfer VT, T. Staake. Economic assessment of photovoltaic battery systems based on household load profiles. Applied Energy. 2018;223:229-48.